

Design of Ultra-wide Band-pass Filter Based on Metamaterials Applicable to Microwave Photonics

Chongmin Lee, Wooseok Shim, Yong Moon*, and Chulhun Seo

*School of Electronic Engineering, College of Information Technology, Soongsil University,
511 Sangdo-dong, Dongjak-gu, Seoul 156-743, Korea*

(Received May 3, 2012 : revised June 18, 2012 : accepted June 18, 2012)

We designed an ultra-wide band-pass filter applicable to microwave reflectometry for KSTAR (Korea Superconducting Tokamak Advanced Research) and to microwave photonics. The proposed ultra-wide band-pass filter exhibits a metamaterial structure characterized by a wide band, low insertion loss, and high skirt selectivity. The proposed filter is applied to enhance the linearity of reflectometry at the output of a VCO (voltage controlled oscillator). The pass-band of the proposed filter is observed at 18~28 GHz, and the out-of-band rejection is below 20 dB. Further, we constructed an unwrapped negative phase of $S(2, 1)$ to verify the characteristics of the metamaterial. The under- and upper-band at lower limits of the pass-band are left- and right-handed, respectively. The group delay of the filter is less than 0.5 ns.

Keywords : Ultra wide band, Band pass filter, Metamaterial, Unwrapped phase, Group delay
OCIS codes : (160.3918) Metamaterials; (350.3618) Left-handed materials; (120.2440) Filters; (350.4010) Microwaves; (230.7020) Traveling-wave devices

I. INTRODUCTION

The NFRI (National Fusion Research Institute) recently succeeded in maintaining a condition of H-mode plasma for 7s in KSTAR. A diagnostic system of visible rays and microwaves is used to diagnose the density of ions under plasma conditions in a tokamak such as KSTAR.

A microwave diagnostic system consists of a VCO, a mixer, an antenna, a band-pass filter, and a divider, as shown in Fig. 1 (a). Fig. 1 (b) shows the microwave diagnostic system in the KSTAR tokamak receiving 18~28 GHz of oscillation frequency generated by the VCO. This oscillation frequency is multiplied four times by a frequency multiplier, resulting in a final output frequency of 72~112 GHz.

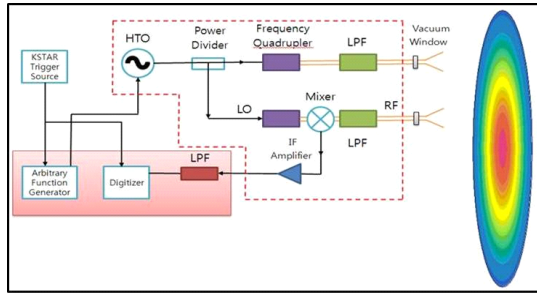
The output signals radiated through the antenna into the tokamak are reflected by ions bonded in the plasma. The reflected signals undergo a Doppler shift because of the difference in the ion density. Finally, we obtain information such as density of ions, internal temperature of the Tokamak, and noise from the dust. We can use this information to control the tokamak.

In this study, we investigate the use of a band-pass filter to suppress certain harmonics at the output of the VCO. The harmonics introduce uncertain information, then the radiated signal returns to the receiver stage of the reflectometry system. Therefore, the microwave diagnostic system requires an ultra-wide band-pass filter to suppress the yielded harmonics at the output of the VCO, which passes frequencies in the 18~28 GHz band and stops all out-of-band frequencies. Finally, we expect to enhance a linearity of reflectometry by using the proposed ultra-wide band-pass filter.

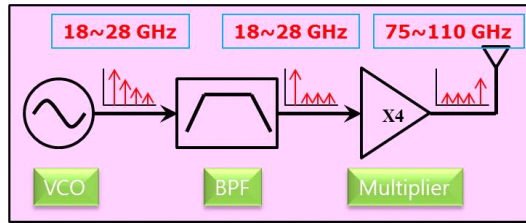
We applied a metamaterial structure to achieve flatness and a superior skirt figure for the ultra-wide pass band. The metamaterial structure operates in the long-wavelength regime, where the lattice does not need to be periodic and the structure is homogeneous. Consequently, the refractive properties of the metamaterial are determined by the nature of the unit cells. These cells are metamaterial composed of sub-wavelength elements that allow the structure to act as an effective medium, with negative permittivity and permeability values at the frequencies of interest. The properties of such media were already studied by Veselago [1] over

*Corresponding author: moony@ssu.ac.kr

Color versions of one or more of the figures in this paper are available online.



(a)



(b)

FIG. 1. Block diagram of (a) microwave reflectometry for KSTAR, (b) analyzed spectrum and output frequency at key-part.

30 years ago. Due to the simultaneous negative values of ϵ and μ , the wave vector k and vectors E and H (the electric- and magnetic- field intensities, respectively), known as triplet, yield the anti-parallel phase and group velocities, or backward-wave propagation.

Pendry [2] experimentally verified the variant structures in the microwave region. If the excitation electric field E is parallel to the axis of the rod medium, the propagated wave is stopped in the spatial frequency band and it exhibits negative permittivity. Further, if the excitation magnetic field H is perpendicular to the plane of the split-ring resonators, the propagated wave is stopped in the spatial frequency band and it exhibits negative permeability [3, 4].

II. DESIGN OF THE ULTRA-WIDE BAND-PASS FILTER

We have designed a theoretical $\lambda/4$ short circuit resonator to achieve maximum flatness for the proposed ultra-wide band-pass filter. We used an Ansoft HFSS (high frequency structure simulator) tool to simulate this circuit.

Figure 2 depicts the structural parameters for the design and layout of the proposed ultra-wide band-pass filter. The proposed filter in this paper consists of Transmission Line (TL), shunt branch with via-hole on the top plane and CSRR cells on the bottom plane (GND plane). The first and last $\lambda/4$ TLs (transmission lines) define the central pass band, and the middle three $\lambda/8$ TLs define the low- and high- cutoff frequencies. The total wavelength of the proposed ultra-wide band-pass filter is 1λ , where f_0 is 18.5

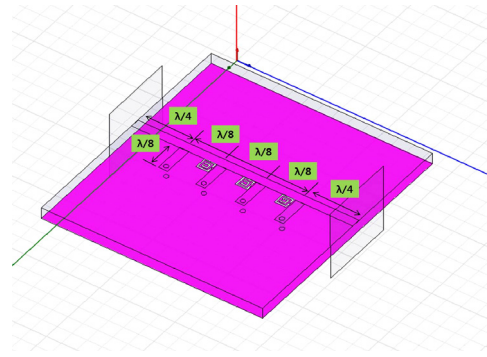


FIG. 2. Layout of the proposed ultra-wide band-pass filter.

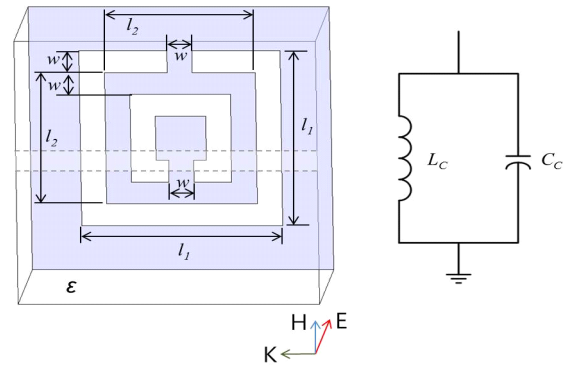


FIG. 3. Layout and equivalent circuit of the CSRR structure. Grey zones represent the metallization with GND and dash line is a transmission line.

GHz. A short circuit of the $\lambda/8$ TL in the shunt bridge is responsible for the flatness of the pass band.

We suggested the use of a CSRR (complementary split ring resonator) in order to enhance the flatness of the pass band. On the other hand, a metamaterial is applied to an ultra-wide band-pass filter with a low return loss of less than -10 dB to maintain the flatness of the pass band over a wide range. Further, the position of the CSRRs has an effect on the matching and shape of the stop-band, given that it alters the field distribution [4]. The layout and equivalent circuit of the CSRR cell, which is etched into the ground plane underneath the Transmission Line, is shown in Fig. 3. As shown in Fig. 3, the CSRR essentially behaves as an electric dipole that can be excited by an axial electric field, where ' C_c ' is the capacitance of the inner gray square disk surrounded by a ground plane at a distance ' w ' of its edge, ' $L_c = 2\pi(l_2 - w)L_{pul}$ ' and L_{pul} is the per unit length inductance of the connecting the inner disk to the ground [5].

The proposed CSRR cell exhibits shunt-parallel resonance characteristics in 2D (two dimensions). The resonance characteristic of the CSRR is varied with a width of the slots and the gap between the slots [6, 7], where ' w ' is 0.1 mm, ' l_1 ' and ' l_2 ' are 0.8 mm and 0.4 mm, respectively and ' ϵ ' is 3.2.

The simulation results of the proposed ultra-wide band-pass filter are shown in Fig. 4. In Fig. 4 (a), the pass band is 18~28 GHz. The insertion loss and return loss are less than 1 dB and greater than 10 dB, respectively. In addition, the group delay is less 0.5 ns in the pass band, as shown in Fig. 4 (b). Further, the difference between slow and fast group delay of pass band is less than 0.04 ns. Fig. 4 (c) shows the unwrapped negative phase of $S(2,1)$ of the proposed ultra-wide band-pass filter, using which the characteristics of the metamaterial can be verified. It exhibits left- and right- handed range. It can be easily verified that $-\angle S(2,1) < 0$ (phase advance) for $f < f_0$ (Left-Handed range) and $-\angle S(2,1) > 0$ (phase lag) for $f > f_0$ (Right-Handed range), as shown in Fig. 4 (c) [6].

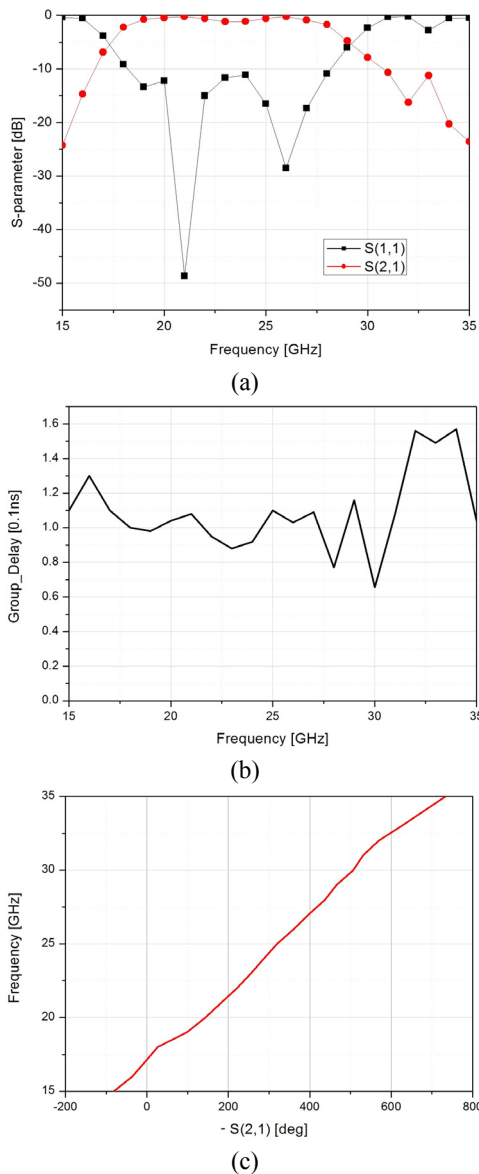


FIG. 4. Simulation result of the proposed ultra-wide band-pass filter: (a) S-parameter, (b) group delay, (c) unwrapped negative phase of $S(2,1)$.

III. FABRICATION AND MEASUREMENT OF ULTRA-WIDE BAND-PASS FILTER

We fabricated an ultra-wide band-pass filter using a Taconic TLC-32 with a permittivity 3.2. Fig. 5 shows the fabricated

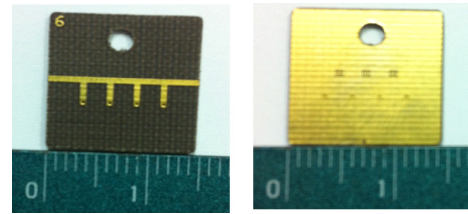


FIG. 5. Substrate of the proposed ultra-wide band-pass filter.

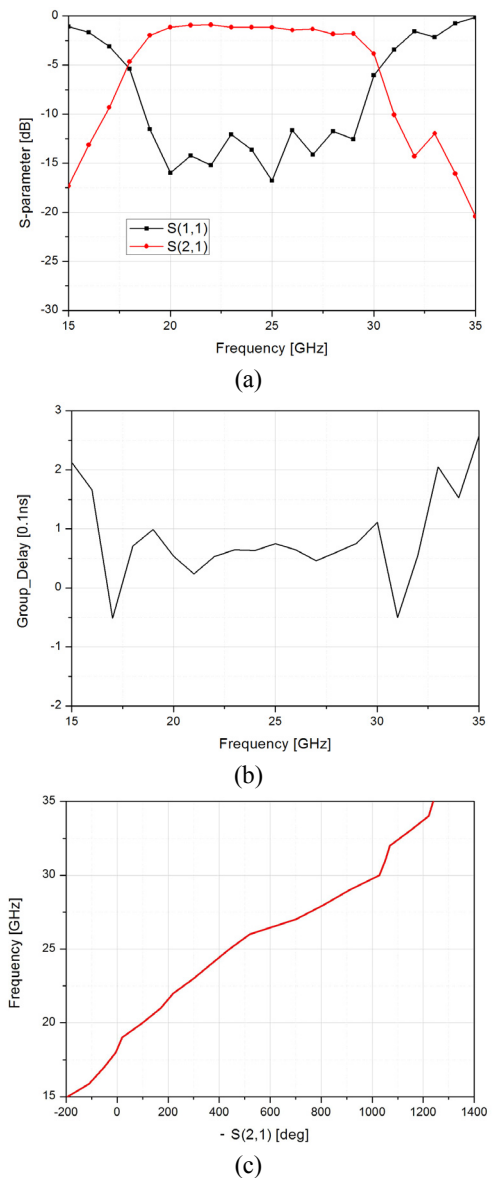


FIG. 6. Measurement of the proposed ultra-wide band-pass filter: (a) S-parameter, (b) group delay, (c) unwrapped negative phase of $S(2,1)$.

TABLE 1. Compare the proposed filter with other filters in K-band

| | Frequency (Bandwidth) [GHz] | Insertion loss [dB] | Return loss [dB] | Group delay [ns] |
|-----------|-----------------------------|---------------------|------------------|------------------|
| [8] | 16.5-19.5 (3) | < 1.3 | > 16.5 | - |
| [9]* | 24-24.25 (0.25) | < 0.3 | > 15 | - |
| [10] | 20-20.3 (0.3) | < 0.1** | > 20 | - |
| [11] | 21-25.2 (432) | < 1.3 | > 9.5 | - |
| This work | 18.5-28.5 (10) | < 2 | > 10 | 0.5 |

* Only simulation results, ** Only ripple characteristic

substrate. An Agilent 8510C (vector network analyzer) is used to measure the fabricated ultra-wide band-pass filter. The results of the measurement are shown in Fig. 6 and are similar to the simulation results. The pass band ranges from 18.5 GHz to 28.5 GHz; those results are only slightly different from the simulation measurement results. The insertion loss and return loss are less than 2 dB and greater than 10 dB, respectively. The out-of-band rejection is below 20 dB. Further, the pass band shows superior flatness because the ripple is below 1 dB.

The group delay is shown in Fig. 6 (b); it is 0.5 ns, which is the same as the simulation result. The unwrapped negative phase of S(2,1) is shown in Fig. 6 (c). The fabricated ultra-wide band-pass filter shows left-handed range below the low cutoff frequency and right-handed range above the low cutoff frequency as the simulation result [6].

The proposed ultra-wide band-pass filter and other filter in K-band are compared in Table 1. The proposed ultra-wide band-pass filter has superior bandwidth than other filters.

IV. CONCLUSION

In this paper, we propose an ultra-wide band-pass filter to use in the KSTAR diagnostic system. We have been improved flatness and group delay characteristics by using a theoretical $\lambda/4$ short circuit to achieve maximum flatness and metamaterial structure.

The proposed ultra-wide band-pass filter is designed to pass band over 10 GHz from 18 GHz to 28 GHz. The insertion loss, return loss, and group delay are less than 2 dB, greater than 10 dB, and 0.5 ns in the pass band, respectively. We expect to suppress harmonics over 20 dB in the stop band using the proposed filter.

Here, we have studied the proposed ultra-wide band-pass filter by applying a metamaterial in the microwave band. The advantage of using a metamaterial is that it maintains flatness in the pass band as an effect on the matching and

the shape of the stop band. Therefore, we expect to apply the proposed filter in the microwave band as well as in the photonics band for achieving good flatness and short group delay.

ACKNOWLEDGMENT

This work was supported by the Soongsil University Research Fund of 2009.

REFERENCES

1. V. G. Veselago, "The electrodynamics of substances with simultaneously negative values of ϵ and μ ," *Sov. Phys. Usp.* **10**, 509-514 (1968).
2. J. B. Pendry, "Negative refraction makes perfect lens," *Phys. Rev. Lett.* **85**, 3966-3969 (2000).
3. D. M. Pozar, *Microwave Engineering*, 3rd ed. (Wiley, Danvers, MA, USA, 2005), p. 427.
4. A. Ali and Z. Hu, "Metamaterial resonator based wave propagation notch for ultrawideband filter applications," *IEEE Trans. Antennas Propag.* **7**, 210-212 (2007).
5. J. D. Baena, J. Bonache, F. Martin, R. M. Sillero, F. Falcone, T. Lopetegi, M. A. G. Laso, J. Garcia-Garcia, I. Gil, M. F. Portillo, and M. Sorolla, "Equivalent-circuit models for split-ring resonators and complementary split-ring resonators coupled to planar transmission lines," *IEEE Trans.* **53**, 1451-1461 (2005).
6. C. Caloz and T. Itoh, *Electromagnetic Metamaterials: Transmission Line Theory and Microwave Applications* (Wiley, Danvers, MA, USA, 2006), pp. 59-105.
7. S. M. Mok and S. Kahng, "Widened bandwidth of a metamaterial ZOR patch antenna with a short-circuited ring," in *Proc. Antennas and Propagation in Wireless Communications, 2011 IEEE-APS Topical Conference* (Torino, Italy, 2011), pp. 398-400.
8. B. Zheng, Z. Zhao, and Y. Lv, "Design of k-band oversized floded half mode substrate integrated waveguide (OFHMSIW) filter with high selectivity," in *Proc. Electronics, Communications and Control (ICECC)* (Las Vegas, NV, USA, 2011), pp. 2000-2002.
9. X. Li, J. Gao, C. L. Law, and S. Aditya, "K band two $\lambda/2$ resonators micromachined filter design," in *Proc. ICICS-PCM 2003* (Singapore, 2003), vol. 2, pp. 1106-1109.
10. A. A. Sulaiman, M. F. Ain, S. I. S. Hassan, A. Othman, M. A. Othman, R. A. Majid, M. Z. Saidin, M. H. A. Hamid, M. H. Jusoh, Z. I. Khan, N. H. Baba, R. A. Awang, N. A. Zakaria, and M. K. A. Mahmood, "Design of hairpin band pass filters for k-band application," in *Proc. RF and Microwave Conference 2008* (Kuala Lumpur, Malaysia, 2008), pp. 23-26.
11. J. Guo, L. Sun, S. Zhou, Y. Bian, J. Wang, B. Cui, C. Li, X. Zhang, H. Li, Q. Zhang, X. Wang, C. Gu, and Y. He, "A 12-pole k-band wideband high-temperature superconducting microstrip filter," *IEEE Trans. Appl. Supercond.* **22**, 1500106 (2012).